Available online at www.sciencedirect.com
ScienceDirect
European Journal of Pharmaceutics and Biopharmaceutics 64 (2006) 326–335
European Journal of Pharmaceutics and Biopharmaceutics
www.elsevier.com/locate/ejpb

Research paper

Visualizing the conversion of carbamazepine in aqueous suspension with and without the presence of excipients: A single crystal study using SEM and Raman microscopy

F. Tian [a], N. Sandler [a,*], K.C. Gordon [b], C.M. McGoverin [b], A. Reay [c], C.J. Strachan [d], D.J. Saville [a], T. Rades [a]

[a] School of Pharmacy, University of Otago, Dunedin, New Zealand
[b] Department of Chemistry, University of Otago, Dunedin, New Zealand
[c] Department of Geology, University of Otago, Dunedin, New Zealand
[d] Division of Pharmaceutical Technology, Faculty of Pharmacy, University of Helsinki, Finland

Received 8 February 2006; accepted in revised form 24 May 2006
Available online 3 June 2006

Abstract

Visual observations of the hydration process of single carbamazepine (CBZ) crystals in water and in various excipient solutions [(1% w/v) – hydroxypropyl cellulose (HPC), poly(vinyl pyrrolidone) (PVP), sodium carboxymethylcellulose (CMC) at pH 7.5 and 3.0, and polyethylene glycol (PEG)] using scanning electron microscopy (SEM) are reported in this paper. Raman microscopy was used to confirm the chemical structures of the unconverted CBZ and the CBZ dihydrate (DH) needles. It was found that defect structures were a more important driving force than the nature of crystal faces for the initiation of the hydration, but face differences became obvious after 6 h immersion. The biggest crystal face grown from methanol, (100), was the slowest one to be covered with DH needles. A comparison of the molecular arrangements along the three crystal faces [(100), (010) and (001)] was carried out using crystal structure visualization software, and fewer polar groups exposed on the (100) face than on the (001) and (010) faces were found, explaining the comparatively weak interaction of the (100) face with water during hydration. Furthermore, investigation of the influence of excipients on the hydration of CBZ showed that both HPC and PVP strongly inhibited conversion, and no conversion of CBZ to DH was found after 18 h immersion in water. PEG and CMC (pH 7.5) were less potent inhibitors than HPC and PVP, and DH needles were observed on all the faces except the (100) face after 18 h immersion. No conversion was detected for the crystal immersed in CMC solution at pH 3.0. This is likely to be caused by the decreased polarity of CMC in water at pH 3.0 (pK_a,cmc = 4.3), and thus a higher surface adsorption of CMC to the CBZ crystals in dispersion. The influence of excipients on the conversion of CBZ observed in this study agreed well with our previous quantitative studies using Raman spectroscopy. In this study, visual observation using electron microscopy has been demonstrated to be a unique and powerful tool to improve our understanding of polymorphic conversions of CBZ in aqueous suspension.

Keywords: Hydration; Carbamazepine; Single crystal; Dihydrate; Scanning electron microscopy; Raman microscopy; Excipient

1. Introduction

Visual characterisation of any solid material is extremely important in drug development. Different microscopic techniques are widely used especially in early stage evaluation of drug candidates when only a limited amount of material is available. Microscopy can be utilised in the evaluation of particle morphology e.g. to build estimations of the particle size distribution, to determine relative crystallinity and often to acquire crystallographic information as well [1].

In order to get qualitative or quantitative information about particle morphology it is often necessary to obtain some appreciation of its three-dimensional (3D) nature.

* Corresponding author. Present address: School of Pharmacy, University of Otago, P.O. Box 913, Dunedin, New Zealand. Tel.: +64 3 479 3984; fax: +64 3 479 7034.
E-mail address: niklas.sandler@stonebow.otago.ac.nz (N. Sandler).

0939-6411/$ - see front matter © 2006 Elsevier B.V. All rights reserved.
doi:10.1016/j.ejpb.2006.05.014

A certain amount of 3D characteristics is often required in order to get qualitative or quantitative information about particle morphology. Depending on how the images are produced different amounts of 3D features can be distinguished; for instance, optical microscopy has a poorer depth of field and lower resolution than scanning electron microscopy (SEM). However, both optical microscopy and SEM are frequently used in the characterisation of pharmaceutical solids and they are often complementary in problem solving. The use of SEM in various applications probing morphology has been reviewed by Newman and Brittain [1]. However, in recent research on drug crystals, polymorphism and polymorphic transitions, SEM images have provided qualitative evidence and the quantification has been provided by other techniques [2–5]. Consequently, the interpretation of occurring phenomena based on measurements with solid-state characterisation techniques, including spectroscopic methods, is often not fully complemented by the use of imaging techniques.

The possible applications of optical microscopy and SEM in crystal studies are numerous including defect characterisation, monitoring of face dependent phenomena, visualization of dissolution mechanisms and interactions between drug crystals and excipients. In this study, the visualization power of SEM is demonstrated in an anhydrate to hydrate conversion study using carbamazepine (CBZ). Light microscopy has been explored for this purpose by Laine and co-workers as early as 1984, where the whole hydration process of CBZ in aqueous suspension and the related mechanism were described based on the images of the CBZ crystals [6]. Later, the conversion kinetics of CBZ polymorphic anhydrate to the DH in aqueous suspension was quantified using X-ray powder diffraction and fluorescence [7,8]. More recently, in 2006, quantitative studies of the conversion of three different CBZ polymorphic forms I, II and III, and also mixtures of forms I and III, to the DH in aqueous suspension were investigated by our group using Raman spectroscopy [9]. Possible conversion mechanisms of the different polymorphic forms to the DH were suggested based on differences in crystal morphology. Interestingly, for all polymorphic forms (particle size 180–250 μm) used in that study, an incomplete conversion after 210 min of dispersion in water was found. This was assumed to be caused by the deactivation of the original surface by a coating of DH crystals, which was also suggested by other authors [6,10]. Such coverage would impede further penetration of water molecules into the core of the unconverted CBZ. The influence of excipients on the conversion kinetics of CBZ polymorphs to the DH was also investigated by our group [11]. It was found that excipients having both low solubility parameters (<27.0 $MPa^{1/2}$) and strong hydrogen bonding groups could inhibit the conversion completely. Such excipients include hydroxypropyl cellulose (HPC) and poly(vinyl pyrrolidone) (PVP). The inhibition ability decreased with increasing solubility parameter, e.g. for sodium carboxymethylcellulose (CMC). Excipients such as polyethylene glycol (PEG) lacking strong hydrogen bonding groups were of poor inhibition ability although they have a low solubility parameter (<21.0 $MPa^{1/2}$). However, even with a better understanding of the conversion kinetics of bulk CBZ power and the influence of excipients on the kinetics based on the quantitative studies described above, questions regarding the hydration process of single crystals remain open: Is surface coverage of DH crystals on the initial CBZ crystals the reason for the observed incomplete conversion of CBZ in water? Is the hydrogen bonding with water in CBZ face-dependent? Do different faces of CBZ interact differently with the different excipients? Recently, SEM was used in the investigation of DH growth on the surface of single CBZ crystals [10] but the focus of data analysis was not on image information from SEM. The efforts of applying imaging techniques on more fundamental investigations have always been limited compared with the use of other techniques such as X-ray powder diffraction, and more recently IR and Raman spectroscopy, which have all been tried in various ways to extract more information from CBZ suspensions [2,5,7–9,12–21]. Therefore, the aim of this study is to apply SEM as a visualization technique to explore the relation between the crystal morphology and the anhydrate-hydrate conversion process. Also, as the growth of the DH crystals is related to molecular interactions between CBZ and water molecules, conversion differences between the important crystal faces are studied and discussed in terms of the molecular arrangements along the crystal faces. Furthermore, the effect of excipients on the conversion of CBZ crystals is investigated.

2. Materials and methods

2.1. Materials

CBZ form III was purchased from Aldrich Chemie (Munich, Germany). Methanol (HPLC grade) was obtained from Merck Ltd. (Palmerston, New Zealand). HPC with a nominal molecular weight of 80,000 and sodium carboxymethyl cellulose (CMC) with a nominal molecular weight of 90,000 were purchased from Sigma Chemical Co. (St. Louis, MO). PVP with a nominal molecular weight of 24,500 and PEG with a nominal molecular weight of 6000 were obtained from BDH Chemicals Ltd. (Poole, England).

2.2. Methods

2.2.1. Growth of single CBZ crystals

Single crystals were grown by cooling a saturated solution of CBZ form III (*p*-monoclinic form) (1 g) dissolved in methanol (15 ml) at 70 °C. The solution was placed intact in a fume hood at room temperature allowing gradual evaporation of methanol.

2.2.2. Immersion of single CBZ crystals

The freshly prepared single CBZ crystals were mounted onto SEM sample holders using a strip of double-sided

tape, and then immersed in distilled water or each excipient solution (1% w/v) separately at room temperature without stirring. The samples were recovered at several predetermined time intervals and then coated for SEM.

2.2.3. Crystal morphology of single CBZ crystals

SEM micrographs were taken of the initial CBZ single crystal, and also of the crystals recovered after immersion. In total, approximately 100 crystals per sample were examined with SEM and typical sample crystals are presented. Samples were sputter coated with a thin layer of gold-palladium under argon vacuum prior to analysis. SEM (Cambridge Instrument, Stereoscan 360) was performed using a 15 kV beam acceleration voltage. Micrographs were recorded using a PGTE Mitsubishi video/copy processor.

The interplanar angles between the faces of a typical CBZ crystal were measured using a two-circle reflecting goniometer, and the Miller indices of the faces were calculated based on the equation which relates the interplanar angles of *p*-monoclinic crystal system to the unit cell parameters reported for CBZ [22].

2.2.4. FT-Raman spectroscopic techniques

The FT-Raman instrument consisted of a Bruker FRA 106/S FT-Raman accessory (Bruker Optik, Ettlingen, Germany) with a Coherent Compass 1064–500N laser (Coherent Inc, Santa Clara, USA) attached to a Bruker IFS 55 FT-IR interferometer, and a liquid nitrogen-cooled D 418 Ge diode detector. Analysis was carried out at room temperature utilising a laser wavelength of 1064 nm (Nd:YAG laser) and a laser power of 105 mW. Back-scattered radiation was collected at an angle of 180°. Samples of CBZ and the DH powder were measured in aluminum cups and 16 scans were averaged for each sample at a resolution of 4 cm^{-1}. Sulfur was used as a reference standard to monitor the wavenumber accuracy. OPUS™ 5.5 (Bruker Optik, Ettlingen, Germany) was used for all spectral analysis.

FT-Raman microscopy (Ramanscope II Bruker Optik, Ettlingen, Germany) was also used for qualitatively determining the changes of the crystal during hydration. The optical and Raman images were obtained using a 40× objective, and Raman spectra were acquired using 16 scans at a laser power of 500 mW. There was no visual sign of physical or chemical changes after irradiation. Data collection, stage control and data processing were preformed using software OPUS™ 5.5 (Bruker Optik, Ettlingen, Germany).

3. Results and discussion

3.1. Characterisation of the initial single CBZ crystal

The morphology of a typical CBZ crystal and the Miller indices of three faces [(100), (001) and (010)] are shown in Fig. 1.

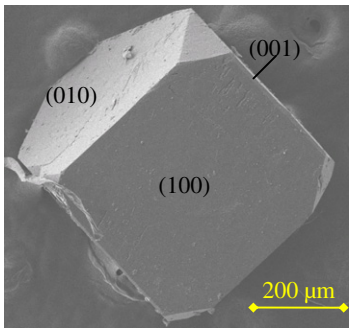

Fig. 1. Morphology of a typical CBZ crystal and Miller indices of three faces.

3.2. Hydration of CBZ crystals

3.2.1. SEM

Fig. 2(a–c) show the SEM images of three selected single crystals (left) and details of their respective surfaces at a higher magnification (right). The magnified area is indicated by a rectangle in the micrographs on the left side. All the crystals in Fig. 2 were immersed in water for less than 1 h. As described by Laine and co-workers, the morphology of DH crystals resembled clusters of whiskers [6]. The obvious morphological differences between CBZ anhydrate (form III) and the DH greatly facilitate the detection of the starting point of the hydration as well as the whole hydration process (see below). As indicated by the arrows in Fig. 2, DH needles could be observed at surface defect structures of each crystal after less than 1 h immersion in water. However, for the areas without obvious defects, no needles could be seen indicating no conversion. Therefore, the SEM images indicate that the initiation of the hydration process is due to the presence of defect structures and that these are a more important driving force to initiate hydration than the nature of crystal faces. This is plausible as it is widely accepted that the crystal growth behaviour has an extreme dependence on defect structures in the crystallisation process [23].

It was noted that the surface morphology of the whole crystal also changed after 1 h immersion in water compared with their original surface morphology [the magnified surface of the initial crystal is shown in Fig. 3a (right)]. The surfaces eroded and surface roughness increased, which is a clear indication of CBZ dissolving in water (Fig. 2(a–c) (right) and 3(b–c)).

For crystals without any obvious surface defects as shown in Fig. 3a (left), it is hard to predict the starting sites for hydration. However, as the conversion process proceeded (from 0 to 18 h), the surface erosion due to CBZ dissolution increased as shown in the magnified micrographs Fig. 3(b–e) (right). Also, differences in the degree of hydration between faces became clear. As shown in Fig. 3c (left), all faces except (100) and (001) were heavily covered with DH needles after 6 h immersion, whereas in Fig. 3d (left), after another 6 h immersion, needles have also started growing on (100) and (001) faces, but some parts of (100)

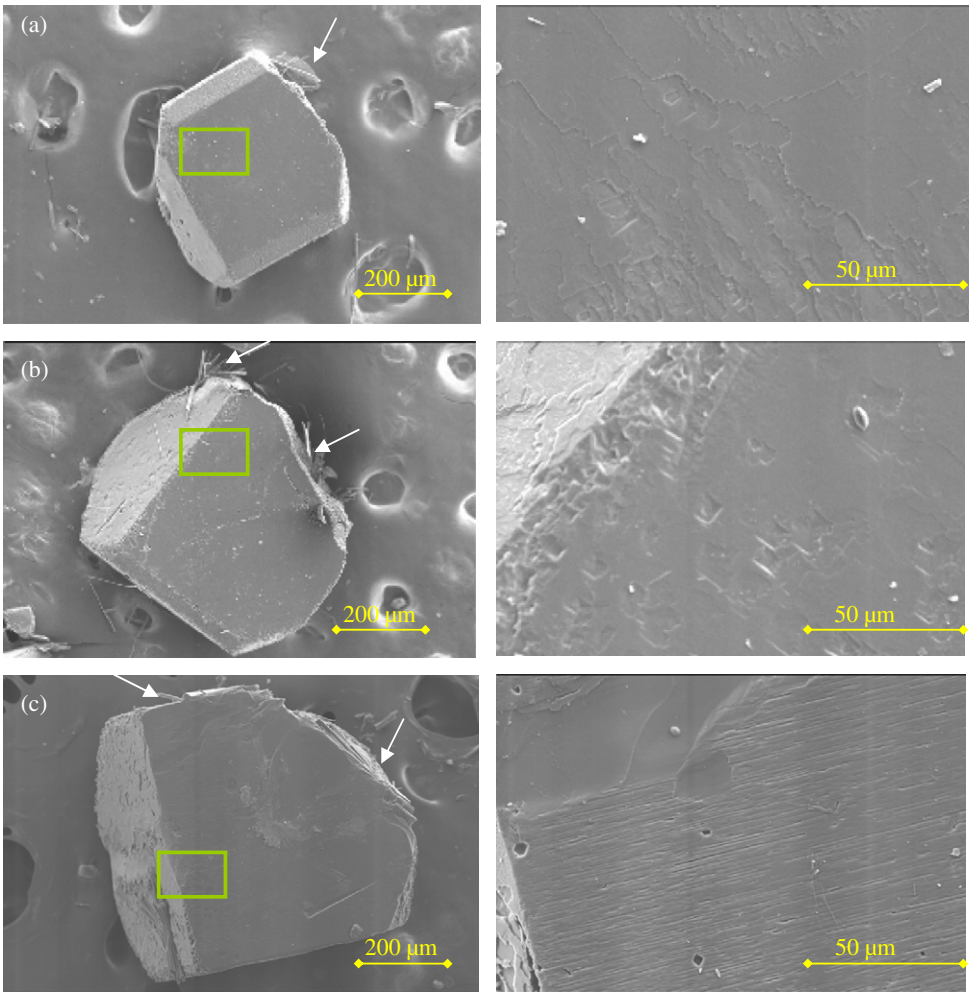

Fig. 2. SEM micrographs of CBZ crystals immersed in water for less than 1 h. The whole crystals are shown on the left (a–c), and the areas indicated by rectangles are shown, respectively, on the right at a higher magnification. Arrows are pointing the areas with DH growth.

face were still without DH. After 18 h immersion, only a very small space of unconverted CBZ could still be observed on the (100) face (Fig. 3e (left)). Therefore, the (100) face showed the slowest conversion to DH needles. It has been shown that in crystal growth the largest faces form when the crystal phase molecules do not strongly interact with solvent; strongly interacting faces tend to be smaller in size [24,25]. Therefore, for the single crystals (grown from methanol), the largest face, (100), should be the one interacting least with the solvent molecules (methanol). Since methanol and water are both polar, protic solvents [26], the face interacting least with methanol should also be the most inactive one in water. This prediction agrees with the electron microscopical observations in this study (Fig. 3). It is possible that the formation of DH nuclei on the (100) face is greatly hampered by its slow dissolution (since it is the weakest face to interact with water). It is also likely that the dissolved CBZ from this face is supplied to the sites where DH nuclei have already formed to promote whiskers growth there. This also explains why the DH needles arrange in a fan-like shape as they mainly grew from a few DH nuclei which worked as the centre points for the growth and then spread to the surrounding areas. Interestingly, [6] also described such orientated growing structure of DH (clusters of whiskers) and mentioned that this orientation could be an important factor for the DH growth.

It can also be seen in Fig. 3e (left) that all the faces of the initial CBZ were finally covered with DH needles. This further confirmed the assumption raised in our previous study that the incomplete conversion of CBZ polymorphs was due to the surface coverage of the DH formed slowing down the conversion process [9]. [10] have not reported any visual evidence for face differences during the hydration of single CBZ crystals. However, our results showed a clear difference between the (100) face and the other faces.

The chemical structures of CBZ and its dimer (present in the crystalline form of CBZ) are shown in Fig. 4a and b, respectively (the possible hydrogen binding sites of CBZ are indicated by the asterisks*). It is well known that the formation of the DH is due to the interaction of the hydrogen bonding groups of CBZ and water molecules [27,28]. The slower hydration rate of the (100) face on the CBZ crystal compared with the other faces also indicated its

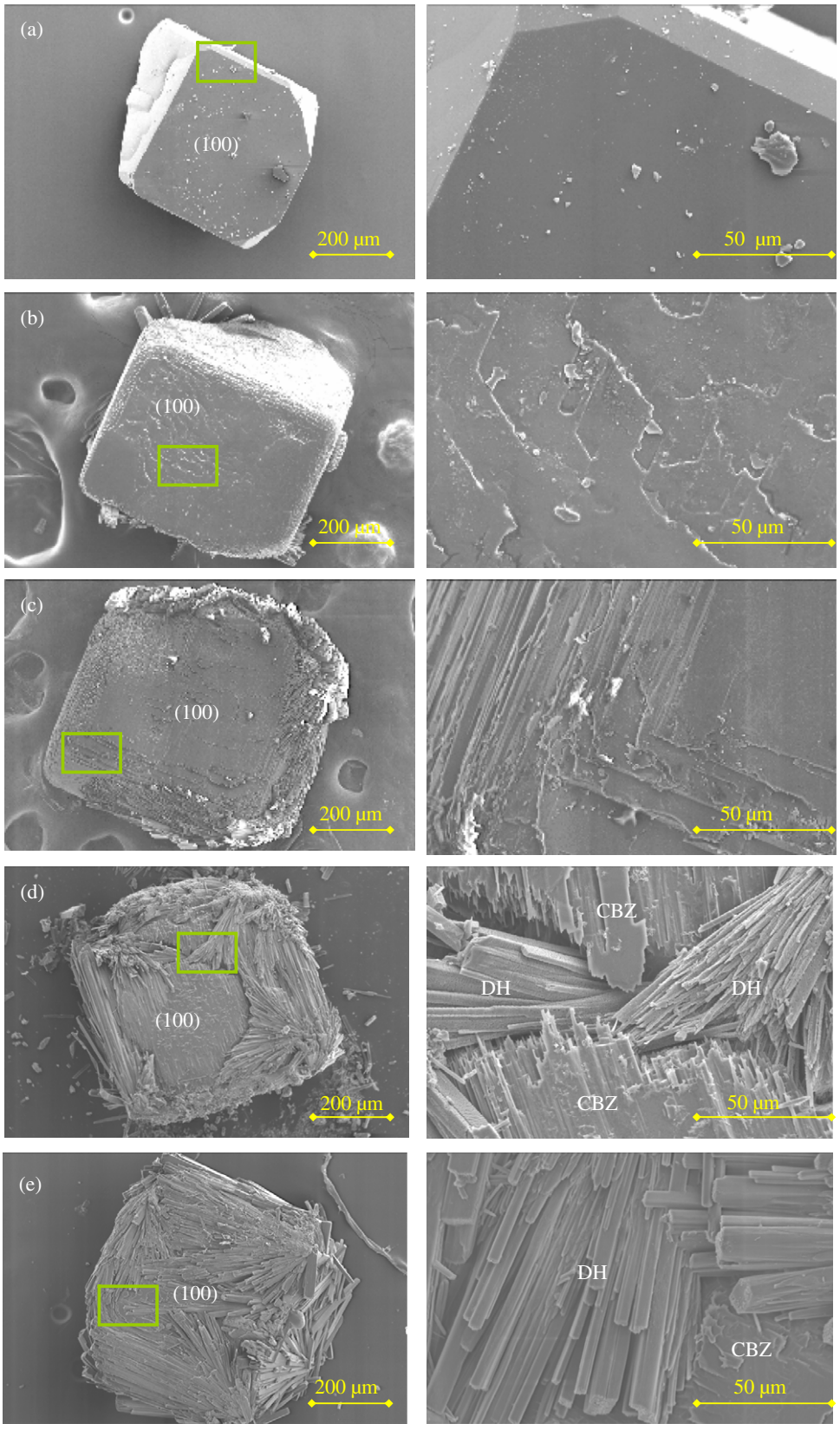

Fig. 3. SEM micrographs of CBZ crystals during the hydration process: (a) initial CBZ crystal; (b) immersed in water for 3 h; (c) immersed in water for 6 h; (d) immersed in water for 12 h; (e) immersed in water for 18 h. The whole crystals are shown on the left (a–e), and the areas indicated by rectangles are shown on the right at a higher magnification.

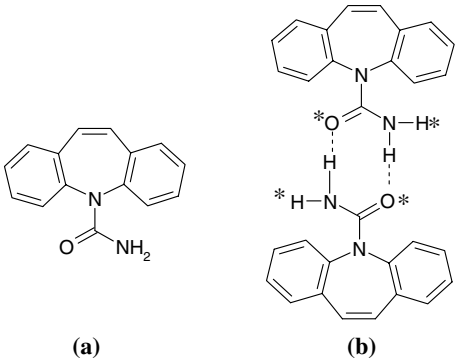

Fig. 4. Chemical structures of CBZ (a) and its dimer (b).

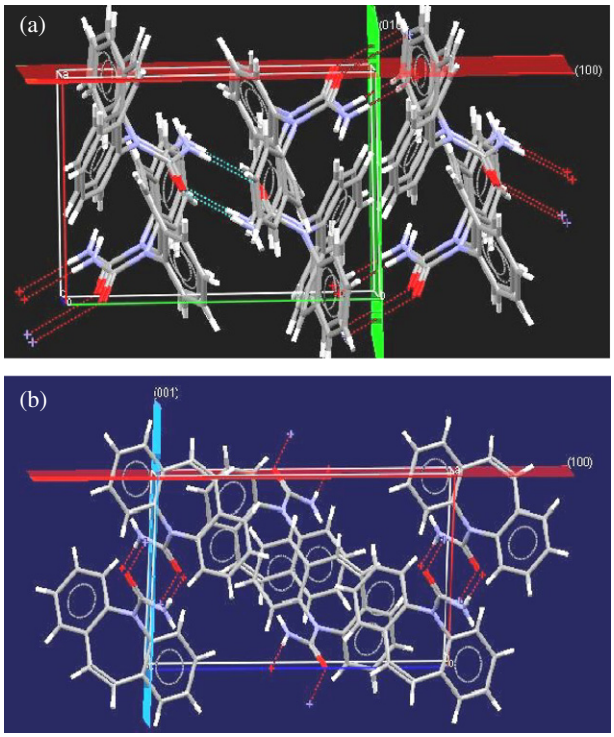

Fig. 5. Molecular structure of the two faces [(100) and (010)] (a), and of the two faces [(100) and (001)] (b).

poorer hydrogen bonding abilities. These are primarily due to the CO and NH_2 groups, which are fewer in number and/or less exposed at the (100) face.

To better understand the molecular arrangement along the faces of the CBZ single crystal, Fig. 5a and b show the [(100) and (010)] faces, and [(100) and (001)] faces, respectively (illustrated with the crystal structure visualization software, Mercury 1.4.1, CCDC, UK). These figures can be used to explore the difference in hydrogen bonding groups between these three faces of the CBZ crystal. In Fig. 5a, the (010) face (green) is characterised by polar NH groups and non-polar CH groups from the ring structures, whereas the (100) face (red) is mainly characterised by non-polar hydrocarbon (CH) groups from the ring structures of the CBZ molecule. Although polar carbonyl groups are present, these are not as frequently occurring as the polar NH groups on the (010) face. Also, for the (001) face (blue) in Fig. 5b, both polar NH and carbonyl groups are frequently occurring, indicating the stronger hydrogen bonding ability of the (001) face compared to the (100) face (red).

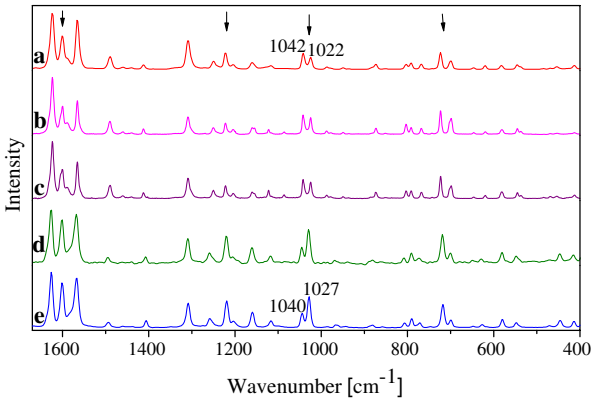

Fig. 7. FT-Raman spectra of: (a) CBZ form III powder; (b) area on the smooth surface of the initial crystal without contacting water; (c) area without needles on the incompletely converted crystal; (d) area covered with needles on the incompletely converted crystal; and (e) CBZ DH powder. Peaks showing obvious differences between CBZ and the DH are indicated by the arrows.

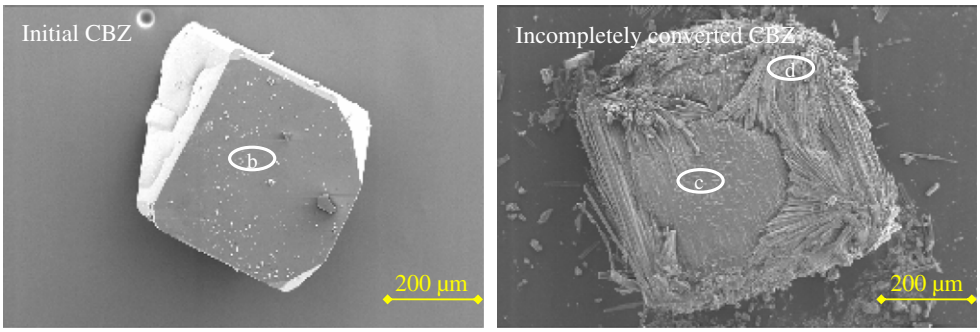

Fig. 6. Micrographs of the surface of CBZ crystals taken by Raman microscopy (40× magnification): ellipse (b) is on the surface of initial CBZ; ellipses (c) and (d) are on the surface of the CBZ recovered from 12 h immersion in water: (c) is the area without any growth of needles, (d) is the area covered with needles.

3.2.2. FT-Raman spectra

The initial CBZ crystal (with no contact to water) shown in Fig. 3a and the incompletely hydrated crystal shown in Fig. 3d were also used for Raman measurements in order to further confirm the chemical structure of the initial CBZ and the needles grown on its surface. Although

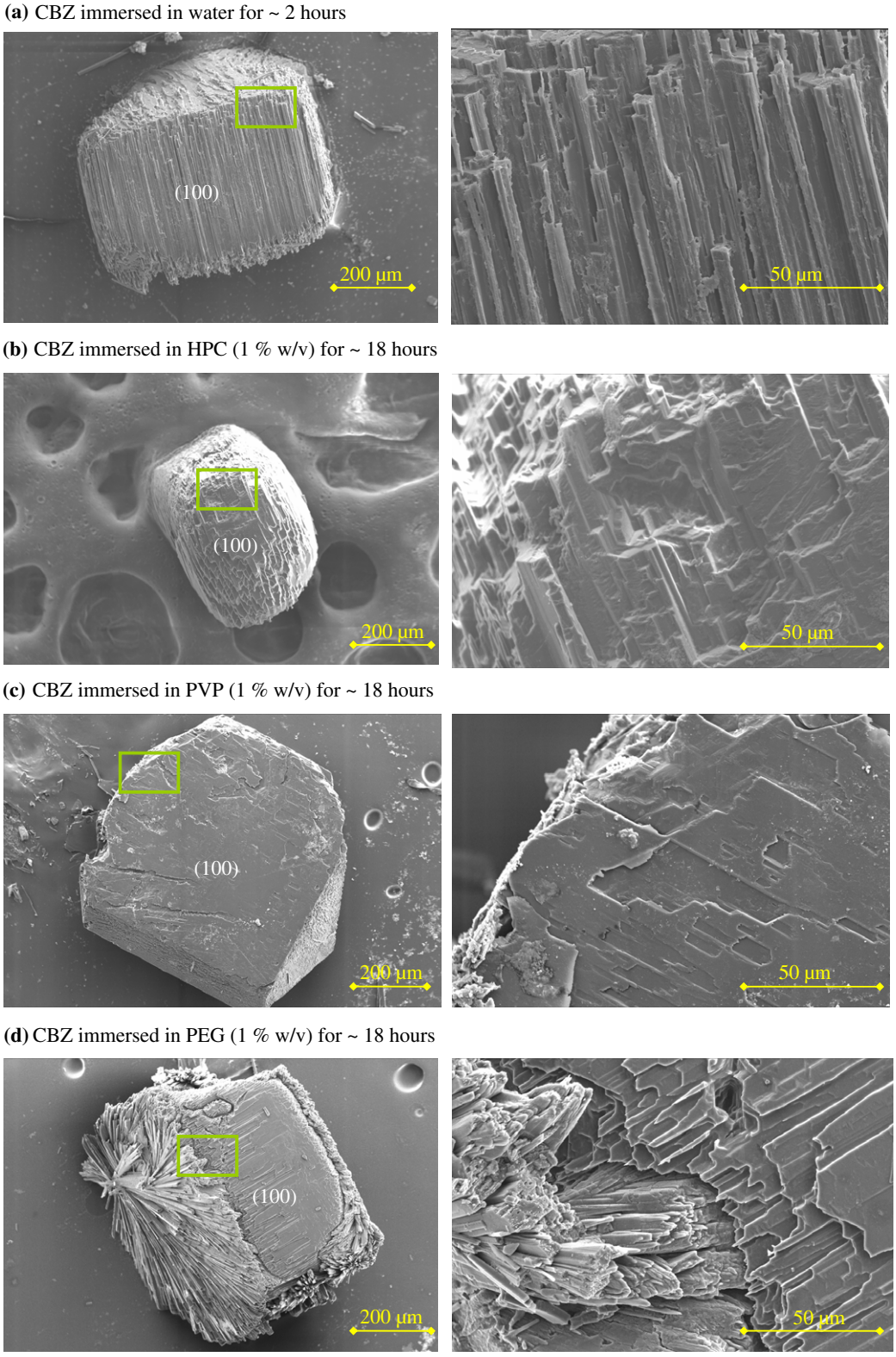

Fig. 8. SEM micrographs of CBZ crystals immersed in water for 2 h (a) and for 18 h (g) and in various excipient solutions (b–f) for 18 h. The whole crystals are shown on the left (a–g), and the areas indicated by rectangles are shown on the right (a–g) at a higher magnification.

(e) CBZ immersed in CMC (1 % w/v, pH = 7.5) for ~ 18 hours

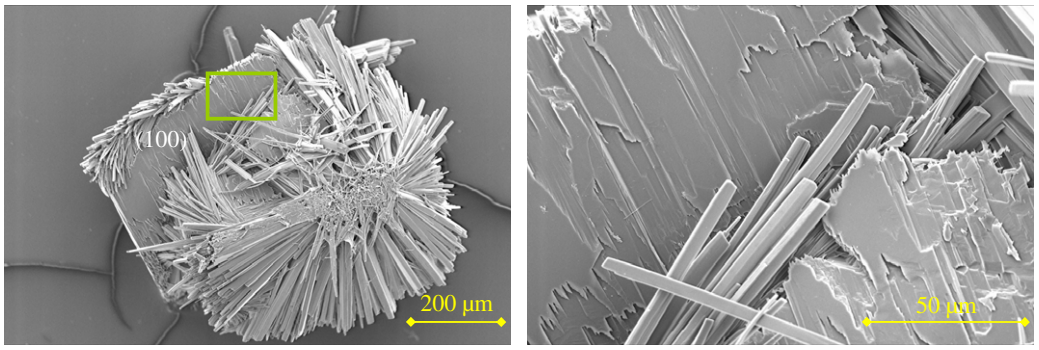

(f) CBZ immersed in CMC (1 % w/v, pH = 3.0) for ~ 18 hours

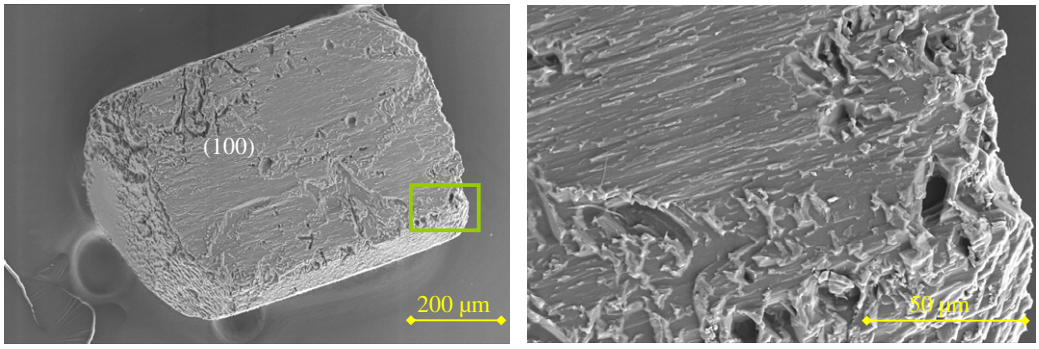

(g) CBZ immersed in water for ~ 18 hours

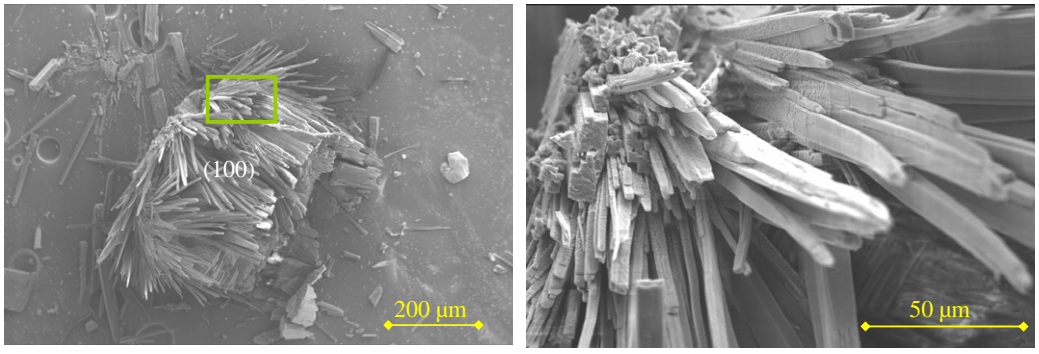

Fig. 8 (*continued*)

FT-Raman has been used in online measurements of the conversion of CBZ to the DH in a microliter fluid cell [29], the growth of needles on the surface of the single CBZ crystals using FT-Raman microscopy presented in this work has not been reported previously.

Fig. 6 shows micrographs of the surface of the crystals shown in Fig. 3a and d taken with a Raman microscope. The areas measured by the Raman laser on the crystal are indicated by the ellipses in Fig. 6, and the labels inside the ellipses (b, c, and d) correspond to the spectra shown in Fig. 7.

The orientation of a crystalline sample can result in intensity changes in Raman spectra [30]. In our studies there are some small intensity differences between the powder sample (which is randomly oriented, Fig. 7a) and the crystalline samples (Fig. 7b and c). A small shoulder at 1588 cm^{-1} due to the stretching of C=C bonds becomes slightly more obvious in the crystalline samples compared to the powder sample. Nevertheless, it is clear that the spectra from the smooth surface at (100) face of the initial CBZ (Fig. 7b) and that of the surface at (100) face without any needles (Fig. 7c) are that of the CBZ form III. Also, the Raman spectrum from the surface covered with needles is similar to that of DH powder (Fig. 7e). Although differences between form III and DH can be observed in the whole spectral range shown in Fig. 7 (as indicated by the arrows), the most distinguished difference is the band pattern at around 1042 cm^{-1} (aromatic C—H bend). The distinct band pattern of DH at 1040 and 1027 cm^{-1} is reproduced in the spectrum of the needles (Fig. 7d). The Raman spectra confirm that the needles grown on the converted CBZ single crystal are DH, and the area without needles coverage is the unconverted CBZ.

3.3. Hydration of CBZ crystals in the presence of excipients

Morphological differences of CBZ crystals immersed in water and various excipient solutions are shown in Fig. 8. Again, the slow dissolution of the CBZ crystals can be clearly seen by SEM as the surface became rough with rigid edges as a function of time. However, these rigid edges did not consist of DH, with its typical fan-like shaped needles. This was also confirmed by FT-Raman microscopy.

The effect of various excipients on the conversion of the CBZ to the DH can also be observed directly from the SEM micrographs in Fig. 8. All the excipients – HPC, PVP, CMC and PEG retarded the conversion to some extent. Both HPC and PVP showed the highest inhibition ability. They completely inhibited the conversion for 18 h (Fig. 8b and c (left)). Taylor and co-workers have demonstrated that the particle size of CBZ crystals dispersed in a PVP solution decreased indicating the dissolution of the crystals [31]. It has been shown clearly in this study that crystals immersed in the excipients with an inhibitory effect keep dissolving and resulting in a rough surface without any formation of the DH nuclei.

CMC (pH 7.5) and PEG also inhibited the hydration to some extent (Fig. 8d and e (left)), and the (100) face was the slowest face for the DH growth in these solutions. Since CMC is an anionic polymer, a low pH value (3.0) was also used to investigate the pH influence on the hydration. Interestingly, no DH needles could be observed after 18 h immersion (Fig. 8f (left)). Again, the surface roughness of the CBZ crystals increased greatly (Fig. 8f (right)), implying dissolution of CBZ in the CMC solution at pH 3.0 without conversion. This strongly retarded conversion at decreased pH agreed well with the suggestions raised from our previous study. The polarity (degree of ionization) of CMC (pK_a,cmc = 4.3) in water decreases with the decreasing pH (from 7.5 to 3.0), which results in its enhanced surface adsorption to the CBZ crystals in the solution. In general, the SEM findings confirmed our previous quantitative studies [11]. Whilst it is difficult to compare the relative degree of inhibition ability between HPC and PVP, or between CMC (at pH 7.5) and PEG from the SEM micrographs above since the size and shape of the initial crystals immersed in the excipient solutions are not all exactly the same, the structural information is unique to the microscopic investigation, and clarified the quantitative behaviour detected by Raman spectroscopy [11].

4. Conclusions

In this study, the power and potential of SEM in the investigation of pharmaceutical polymorphic conversions has been demonstrated. The hydration phenomena of CBZ were clearly observed with SEM imaging and a plausible explanation for the partial conversion of CBZ to the DH was formed based on the growth characteristics of the DH needles. Also, a better understanding of factors such as defects, face differences, influence of excipients, which are all of importance to the physical stability of CBZ, was gained from SEM images; such insights are not expected to be directly detectable using bulk techniques.

Acknowledgements

Thanks to the New Zealand Pharmacy Education Research Foundation (NZPERF) for the research grants for this project. Thanks also to the School of Pharmacy, University of Otago, for providing a scholarship for FT. Research grants from the Academy of Finland and Finnish Cultural Foundation are acknowledged by NS.

References

[1] A.W. Newman, H.G. Brittain, Particle morphology: optical and electron microscopies, in: H.G. Brittain (Ed.), Physical Characterization of Pharmaceutical Solids, Marcel Dekker, Inc., New York, NY, USA, 1995, pp. 127–156.
[2] S. Luhtala, Effect of sodium lauryl sulphate and polysorbate 80 on crystal growth and aqueous solubility of carbamazepine, Acta Pharm. Nordica 4 (1992) 85–90.
[3] Z. Naima, T. Siro, G.-D. Juan-Manuel, C. Chantal, C. Rene, D. Jerome, Interactions between carbamazepine and polyethylene glycol (PEG) 6000: characterizations of the physical, solid dispersed and eutectic mixtures, Eur. J. Pharm. Sci. 12 (2001) 395–404.
[4] B. Noushin, N. Ali, D. Rassoul, The effect of solvent and crystallization conditions on habit modification of carbamazepine, Daru, J. Faculty Pharm. 9 (2001) 12–22.
[5] S. Sethia, E. Squillante, Solid dispersion of carbamazepine in PVP K30 by conventional solvent evaporation and supercritical methods, Int. J. Pharm. 272 (2004) 1–10.
[6] E. Laine, V. Tuominen, P. IIvessalo, P. Kahela, Formation of dihydrate from carbamazepine anhydrate in aqueous conditions, Int. J. Pharm. 20 (1984) 307–314.
[7] W.W.L. Yong, R. Suryanarayanan, Kinetics of transition of anhydrous carbamazepine to carbamazepine dihydrate in aqueous suspensions, J. Pharma. Sci. 80 (1991) 496–500.
[8] H.G. Brittain, Fluoresence studies of the transformation of carbamazepine anhydrate form III to its dihydrate phase, J. Pharm. Sci. 93 (2003) 375–383.
[9] F. Tian, J.A. Zeitler, C.J. Strachan, D. J Saville, C.K. Gordon, T. Rades, Characterizing the conversion kinetics of carbamazepine polymorphs to the dihydrate in aqueous suspension using Raman spectroscopy, J. Pharm. Biomed. Anal. 40 (2006) 271–280.
[10] N.K. Rodríguez-Hornedo, D. Murphy, Surfactant-facilitated crystallization of dihydrate carbamazepine during dissolution of anhydrous polymorph, J. Pharm. Sci. 93 (2003) 449–460.
[11] D.J. Saville, F. Tian, K.C. Gordon, C.J. Strachan, J.A. Zeitler, T. Rades, Conversio of carbamazepine polymorphs to the dihydrate in aqueous suspension: inhibition by various excipients, in: Proceedings of the Annual Conference of the Australasian Pharmaceutical Science Association, Melbourne, Australia, 2005.
[12] M.W. Samaha, M.A.F. Gadalla, Solubilization of carbamazepine by different classes of nonionic surfactants and a bile salt, Drug Dev. Ind. Pharm. 13 (1987) 93–112.
[13] M. Otsuka, T. Ohfusa, Y. Matsuda, Effect of binders on polymorphic transformation kinetics of carbamazepine in aqueous solution, Colloids Surf. B: Biointerfaces 17 (2000) 145–152.
[14] M. Otsuka, T. Ohfusa, Y. Matsuda, Effect of environmental humidity on the transformation pathway of carbamazepine polymorphic modifications during grinding, Colloids Surf. B 13 (1999) 263–273.
[15] M. Otsuka, M. Ishii, Y. Matsuda, Effect of surface modification on hydration kinetics of carbamazepine anhydrate using isothermal

microcalorimetry, AAPS PharmSciTech [electronic resource] 4 (2003) E5.
[16] B. Perissutti, F. Rubessa, M. Moneghini, D. Voinovich, Formulation design of carbamazepine fast-release tablets prepared by melt granulation technique, Int. J. Pharm. 256 (2003) 53–63.
[17] I. Katzhendler, S. Ito, S. Itai, K. Yamamoto, Investigating the structure and properties of hydrates hydroxypropyl methylcellulose and egg albumin matrices containing carbamazepine: EPR and NMR study, Pharm. Res. 17 (2000) 1299–1308.
[18] D. Murphy, F. Rodríguez-Cintrón, B. Langevin, R.C. Kelly, N. Rodriguez-Hornedo, Solution-mediated phase transformation of anhydrous to dihydrate carbamazepine and the effect of lattice diorder, Int. J. Pharm. 246 (2002) 121–134.
[19] M. Sarkari, J. Brown, X. Chen, S. Swinnea, R.O. Williams, K.P. Johnston, Enhanced drug dissolution using evaporative precipitation into aqueous solution, Int. J. Pharm. 243 (2002) 17–31.
[20] I. Katzhendler, R. Azoury, M. Friedman, The effect of egg albumin on the crystalline properties of carbamazepine in sustained release hydrophilic matrix tablets and in aqueous solutions, J. Controlled Release 65 (2000) 331–343.
[21] Y. Kobayashi, S. Ito, S. Itai, K. Yamamoto, Physicochemical properties and bioavailability of carbamazepine polymorphs and dihydrate, Int. J. Pharm. 193 (2000) 137–145.
[22] V.L. Himes, A.D. Mighell, W.H. De Camp, Structure of carbamazepine: 5*H*-dibenz[*b*,*f*]azepine-5-carboxamide, Acta Crystallogr. B37 (1981) 2245–2248.
[23] G.R. Ester, R. Price, P.J. Halfpenny, The relationship between crystal growth and defect structure: a study of potassium hydrogen phthalate using X-ray topography and atomic force microscopy, J. Phys. D: Appl. Phys. 32 (1999) A128–A132.
[24] A.S. Myerson, S.E. Decker, W. Fan, Solvent selection and batch crystallization, Ind. Eng. Chem. Process Des. Dev. 25 (1986) 925–929.
[25] C. Stoica, P. Verwer, H. Meekes, P.J.C.M. van Hoof, F.M. Kaspersen, E. Vlieg, Understanding the effect of a solvent on the crystal habit, Cryst. Growth Des. 4 (2004) 765–768.
[26] Y. Marcus, The properties of organic liquids that are relevant to their use as solvating solvents, Chem. Soc. Rev. 22 (1993) 409–416.
[27] J. Han, R. Suryanarayanan, Influence of environmental conditions on the kinetics and mechanism of dehydration of carbamazepine dihydrate, Pharm. Dev. Technol. 3 (1998) 587–596.
[28] L.E. McMahon, P. Timmins, A.C. Williams, P. York, Characterization of dihydrates prepared from carbamazepine polymorphs, J. Pharm. Sci. 85 (1996) 1064–1069.
[29] P.A. Anquetil, C.J.H. Brenan, C. Marcolli, I.W. Hunter, Laser Raman spectroscopic analysis of polymorphic forms in microliter fluid volumes, J. Pharm. Sci. 92 (2002) 149–160.
[30] D.C. Smith, C. Carabatos-Nedelec, Raman spectroscopy applied to crystals, in: I.R. Lewis, H.G.M. Edwards (Eds.), Handbook of Raman spectroscopy: from the Research Laboratory to the Process Line, Marcel Dekker, Inc., New York, NY, USA, 2001, pp. 349–422.
[31] A.K. Salameh, L.S. Taylor, Physical stability of crystal hydrates and their anhydrates in the presence of excipients, J. Pharm. Sci. 95 (2005) 446–461.